Acta Crystallographica Section C
Crystal Structure Communications
ISSN 0108-2701

α-Tris(2,4-pentanedionato-κ^2O,O')-cobalt(III) at 240, 210, 180, 150 and 110 K

Lars S. von Chrzanowski,* Martin Lutz and Anthony L. Spek

Bijvoet Center for Biomolecular Research, Crystal and Structural Chemistry, Utrecht University, Padualaan 8, 3584 CH Utrecht, The Netherlands
Correspondence e-mail: l.vonchrzanowski@chem.uu.nl

Received 17 April 2007
Accepted 9 May 2007
Online 14 June 2007

The crystal structure of the title compound, $[Co(C_5H_7O_2)_3]$, has been investigated by a multi-temperature measurement. In contrast to the isomorphous Al compound, the title compound exists in the studied temperature range as its monoclinic α polymorph (space group $P2_1/c$) and does not undergo a phase transition. Rigid-body **TLS** analyses have been performed and the anisotropic thermal expansion tensor α_{ij} has been determined. The cell axes show a linear expansion behavior with respect to the temperature, but the slope is significantly different. A possible explanation are the different strengths of different intermolecular C—H···O contacts, which run in different crystallographic directions.

Comment

Metal complexes, especially transition metal complexes, play an important role in catalytic processes. Trivalent metal–acetylacetonate (2,4-pentanedionate, acac) complexes are particularly accessible species for studying structure, bonding and ligand coordination in organometallic systems. Polymorphism is well known for these complexes [see *e.g.* Geremia & Demitri (2005) for Mn(acac)$_3$]. In the course of our ongoing studies on these complexes (von Chrzanowski *et al.*, 2006, 2007), we have now determined the crystal structure of Co(acac)$_3$, (I). According to an old nomenclature of Astbury & Morgan (1926), the α polymorph crystallizes in the monoclinic crystal system with space group $P2_1/c$. In our temperature-dependent study of α-Al(acac)$_3$, which is isomorphous with α-Co(acac)$_3$, we observed a phase transition to a new δ polymorph. This phase transition occurs between 150 and 110 K.

To our knowledge, all previous crystallographic investigations of Co(acac)$_3$ were carried out at room temperature. Only the α polymorph of Co(acac)$_3$ has been reported, crystallizing in the monoclinic crystal system with space group $P2_1/c$ (Hon & Pfluger, 1973; Krüger & Reynhardt, 1974). We report here a multi-temperature measurement using the temperatures 240, (I*a*), 210, (I*b*), 180, (I*c*), 150, (I*d*), and 110 K, (I*e*), which are the same as in our previous publication on α-Al(acac)$_3$ (von Chrzanowski *et al.*, 2007).

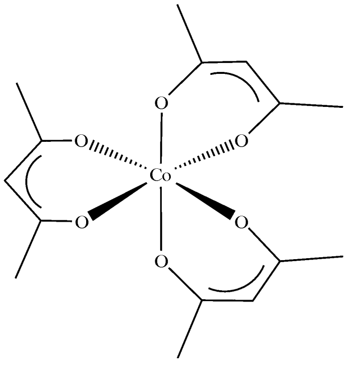
(I)

Co(acac)$_3$ crystallizes as an α polymorph with one independent molecule in the asymmetric unit. No phase transition was observed in the chosen temperature range. The temperature-dependent measurement shows, as expected, a decrease of the anisotropic displacement parameters with decreasing temperature and therefore a decrease of the thermal motion (Fig. 1). The molecule has an approximate noncrystallographic D_3 symmetry, with r.m.s. deviations between 0.114 [for (I*e*)] and 0.122 Å [for (I*a*)] from ideal symmetry (Pilati & Forni, 1998).

It is known that it is difficult to reach the precision of four-circle diffractometer cell parameters from area-detector data (Herbstein, 2000). Two difficulties are noteworthy: (i) the detector is moveable and the detector–crystal distance is highly correlated with the unit-cell volume, and (ii) the precise peak position in rotation direction (time axis) is unknown. In order to overcome some of these difficulties, we carried out temperature-dependent cell-parameter determinations with a fixed detector position and the *Phi*/*Phi-Chi* routine (Duisenberg *et al.*, 2000), which is designed to provide accurate peak positions for the reflections. The crystal used for the above-described intensity measurements was different from that used for the crystal structure determinations. The chosen temperature range was from 290 to 110 K, with steps of 20 K and a cooling rate of 120 K h^{-1}. The cell axes and the cell volume decrease linearly, the *a* axis being the most sensitive to change of temperature. The slope ratio *b*:*c*:*a* is approximately 1:1.8:2.7 (Fig. 2). The cell parameters of the known crystal structure determinations of Co(acac)$_3$ at room temperature are summarized in Table 1. It can be clearly seen that the consistency of these data is much worse than the internal consistency given in Fig. 2, which is based on one single crystal and one diffractometer.

The thermal expansion can also be represented by a symmetrical second-rank tensor, α_{ij}. Calculations for the tensor components, eigenvalues and eigenvectors were performed using the program *ALPHA* (Jessen & Küppers, 1991). 20 reflections were included in the calculation with θ values calculated from the cell parameters. In a monoclinic unit cell, two off-diagonal terms of the tensor are zero and one

DOI: 10.1107/S0108270107022950

axis is parallel to the crystallographic *b* axis. The behavior of the thermal expansion is anisotropic, as can be seen in the values for the tensor components of thermal expansion α_{ij} (Table 2). The largest expansion of Co(acac)$_3$ occurs along the crystallographic *a* axis. This expansion is represented by the eigenvalue of α_3, which is almost parallel to the crystal-

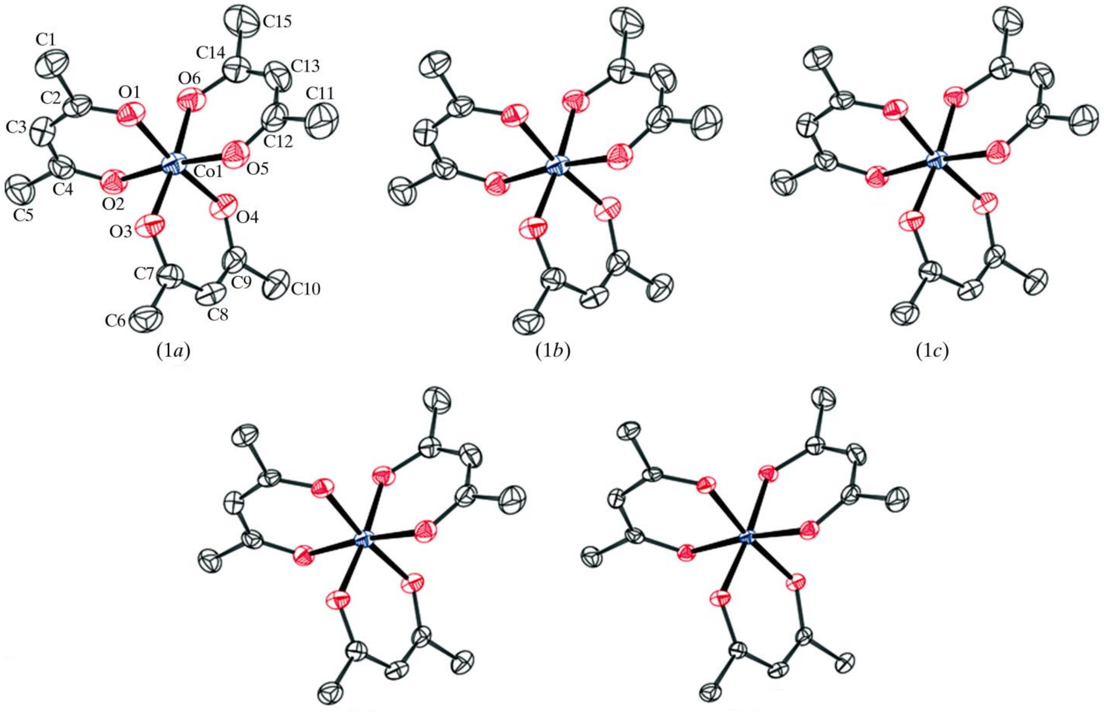

(1*a*) (1*b*) (1*c*)

(1*d*) (1*e*)

Figure 1
Displacement ellipsoid plots and atomic numbering schemes of (I*a*) at 240 K, (I*b*) at 210 K, (I*c*) at 180 K, (I*d*) at 150 K and (I*e*) at 110 K. Ellipsoids are drawn at the 50% probability level. H atoms have been omitted for clarity. All plots are drawn in the same orientation and have the same labeling scheme.

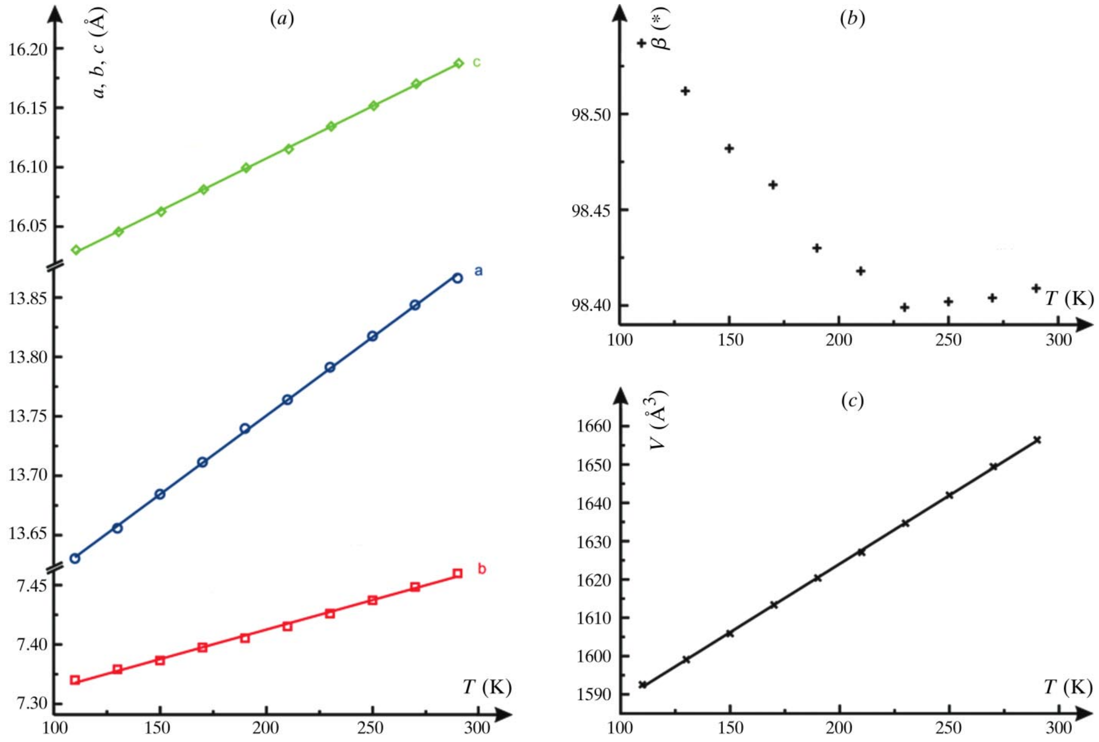

Figure 2
(*a*) Unit-cell lengths *a* (middle line), *b* (lower line) and *c* (top line), (*b*) cell angle β, and (*c*) cell volume as a function of temperature. ($a = 13.486 + 1.32 \times 10^{-3}T$, $b = 7.313 + 0.50 \times 10^{-3}T$, $c = 15.932 + 0.88 \times 10^{-3}T$ and $V = 1552.6 + 0.357T$.)

lographic *a* axis (Table 3). Note that the β angle and its change cannot be determined reliably; for example, a relatively large change in β from 98.5 to 98.6° results in an extremely small change in θ of 0.006° for the 002 reflection.

The anisotropic thermal expansion tensor might give valuable insight into the strengths of intermolecular interactions (Salud *et al.*, 1998; Kitaigorodsky, 1973), while in other cases such a direct relation has been questioned (Boldyreva *et al.*, 1997). It has been noted that acetylacetonate complexes are linked together in the crystal by pure van der Waals interactions (Alekseev *et al.*, 2006), but in the case of α-Co(acac)$_3$, we detect three different C—H$\cdots$O hydrogen bonds of different lengths (Table 4). Methyl H atoms act as hydrogen-bond donors and metal-coordinated O atoms as acceptors, with C—H$\cdots$O angles between 170 and 180° for determinations (I*a*)–(I*e*). The weakest interaction is C11—H11*B*$\cdots$O1^{iii} [from 2.78 Å for (I*a*) to 2.65 Å for (I*e*); symmetry code: (iii) $-x, -y+1, -z+1$], and the vector C11$\cdots$O1^{iii} forms an angle of 33° with the crystallographic *a* axis. The other two interactions, C6—H6*B*$\cdots$O6^{ii} and C1—H1*A*$\cdots$O4^{i}, are shorter [2.53 Å for (I*a*) to 2.47 for (I*e*), and 2.54 Å for (I*a*) to 2.52 Å for (I*e*); symmetry codes: (i) $x, y+1, z$; (ii) $x, -y+\frac{1}{2}, z-\frac{1}{2}$] and form angles of 84 and 72°, respectively, with the crystallographic *a* axis (Fig. 3). The lengths of these hydrogen bonds are linearly dependent on the temperature (Fig. 4). Interestingly, the longest distance, C11$\cdots$O1^{iii}, has the largest slope. This hydrogen bond has the smallest angle to the crystallographic *a* axis, which has also the largest temperature

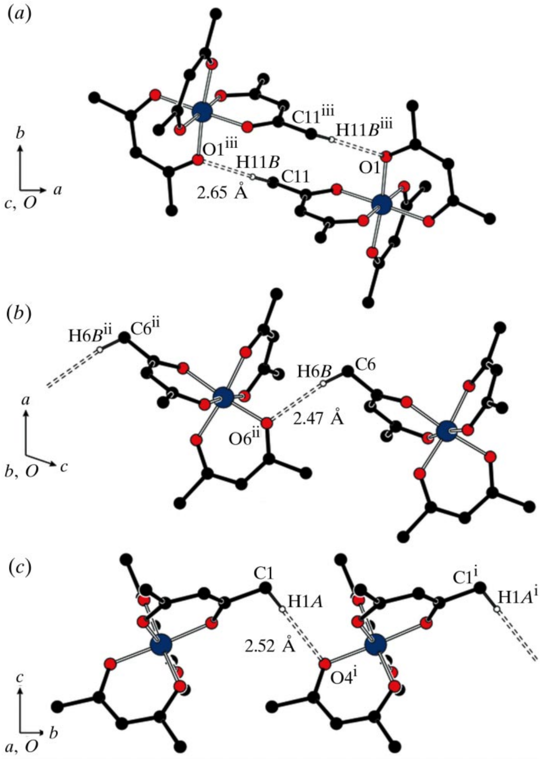

Figure 3
Hydrogen-bond interactions in (I*e*). The C—H$\cdots$O contacts are shown with dashed lines. (*a*) The C1—H11*B*$\cdots$O1^{iii} contact, viewed along the crystallographic *c* axis, (*b*) the C6—H6*B*$\cdots$O6^{ii} contact, viewed along the crystallographic *b* axis, and (*c*) the C1—H1*A*$\cdots$O4^{i} contact, viewed along the crystallographic *a* axis. [Symmetry codes: (i) $x, y+1, z$; (ii) $x, -y+\frac{1}{2}, z-\frac{1}{2}$; (iii) $-x, -y+1, -z+1$.]

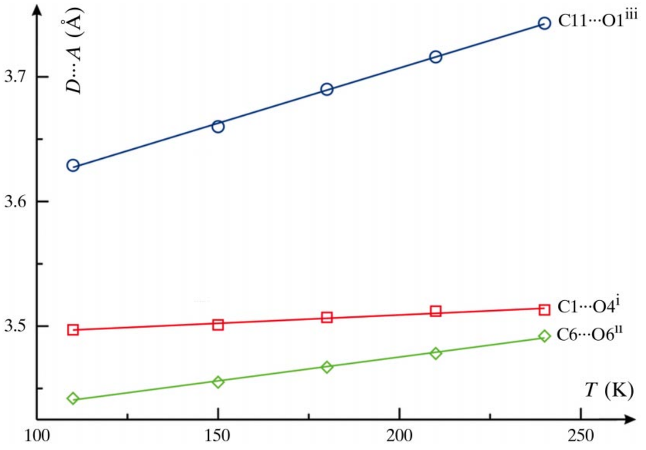

Figure 4
$D\cdots A$ distances for the hydrogen-bond contacts C1—H1*A*$\cdots$O4^{i} (middle line), C6—H6*B*$\cdots$O6^{ii} (lower line) and C11—H11*B*$\cdots$O1^{iii} (top line) as a function of temperature [C1$\cdots$O4^{i} = $3.482 + 0.13 \times 10^{-3}T$, C6$\cdots$O6^{ii} = $3.399 + 0.38 \times 10^{-3}T$ and C11$\cdots$O1^{iii} = $3.530 + 0.89 \times 10^{-3}T$; symmetry codes: (i) $x, y+1, z$; (ii) $x, -y+\frac{1}{2}, z-\frac{1}{2}$; (iii) $-x, -y+1, -z+1$.]

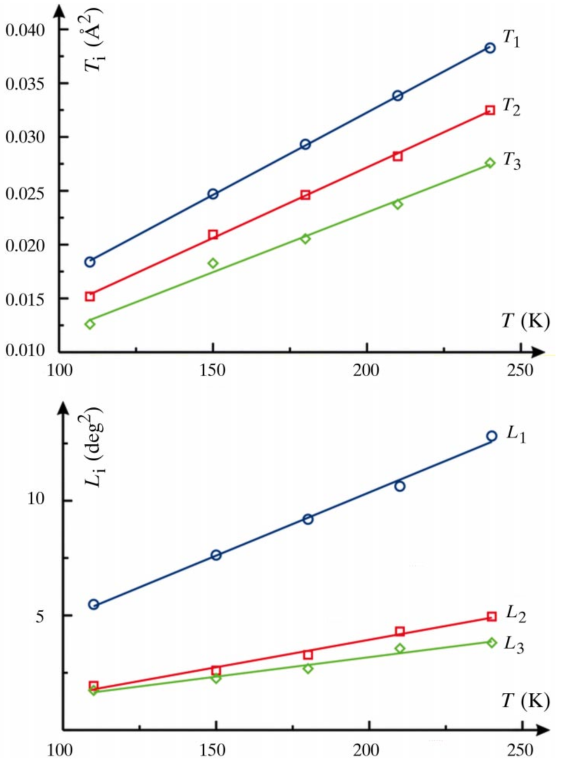

Figure 5
Eigenvalues of translation T_i (top) and libration L_i (bottom) tensors from rigid-body analyses (*PLATON*; Spek, 2003) as a function of temperature. ($T_1 = 1.68 \times 10^{-3} + 0.15 \times 10^{-3}T$, $T_2 = 0.95 \times 10^{-3} + 0.13 \times 10^{-3}T$, $T_3 = 0.76 \times 10^{-3} + 0.11 \times 10^{-3}T$, $L_1 = -0.67 + 0.06T$, $L_2 = -0.86 + 0.02T$ and $L_3 = -0.22 + 0.02T$.)

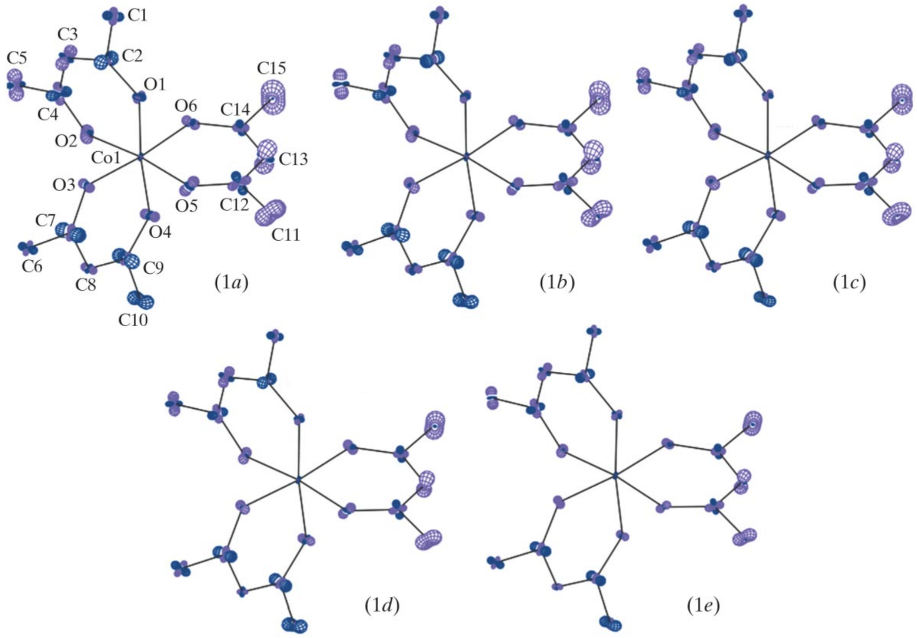

Figure 6
Peanut plots of (I*a*) at 240 K, (I*b*) at 210 K, (I*c*) at 180 K, (I*d*) at 150 K and (I*e*) at 110 K, showing the difference between the measured displacement parameters and the parameters obtained by rigid-body analyses using the program *THMA11* (Schomaker & Trueblood, 1998). A scale factor of 3.08 was used for the r.m.s. surfaces. Darker lines (blue in the electronic version) indicate positive differences and lighter lines (purple in the electronic version) negative differences. All plots are drawn in the same orientation and have the same labelling scheme.

dependence of the cell parameters (see above). The other two hydrogen bonds are approximately in the *bc* plane and have a smaller temperature dependence.

The eigenvalues of the translation **T** and libration **L** tensors obtained from rigid-body analyses (*PLATON*; Spek, 2003) show that the decrease of the thermal motion is linear in the whole temperature range (Fig. 5). The agreement factors of the rigid-body analyses are rather high {R = 0.104–0.129; $R = [\sum(U_{\rm obs} - U_{\rm calc})^2/\sum U^2_{\rm obs}]^{1/2}$}. This situation is similar to that for α-Al(acac)$_3$, where the agreement factors (R = 0.155–0.167) are even higher. The corresponding internal motion is visualized by difference plots (Hummel *et al.*, 1990) between the observed displacement parameters and the rigid-body models (Fig. 6). The nonrigid behavior is mainly expressed by only one acac ligand (C11–C15). This behavior is also observed in the aluminium compound.

Considering the displacement parameters at a particular temperature, the internal motions are also reflected in a relatively large variation of the bond lengths. For example, the Co—O distances range between 1.8746 (18) and 1.8892 (17) Å at 240 K, *viz*. determination (Ia). The corresponding Al—O distances in α-Al(acac)$_3$ for 240 K are 1.8712 (13)–1.8862 (12) Å and show a similar variation (von Chrzanowski *et al.*, 2007). Because octahedral, low-spin Co$^{\rm III}$ with electron configuration d^6 does not express Jahn–Teller distortions (Wiberg, 1985), this variation can only be explained by internal thermal motion. The thermal motion also contributes to a shortening of the Co—O distances (Table 5) of the crystal structure determinations compared with the value of 1.899 Å obtained for Co(acac)$_3$ from high-level density functional theory (6–31G* for C, H, O and triple-ζ for Co) calculations (Diaz-Acosta *et al.*, 2003).

Experimental

Dark-green crystals were obtained by slow evaporation of a solution of the commercially available material (Aldrich) in ethyl acetate at room temperature.

Compound (I*a*), at 240 K

Crystal data

[Co(C$_5$H$_7$O$_2$)$_3$]
M_r = 356.25
Monoclinic, $P2_1/c$
a = 13.8094 (7) Å
b = 7.4331 (4) Å
c = 16.1484 (9) Å
β = 98.430 (3)°
V = 1639.66 (15) Å^3
Z = 4
Mo $K\alpha$ radiation
μ = 1.07 mm^{-1}
T = 240 (2) K
0.23 × 0.15 × 0.05 mm

Data collection

Nonius KappaCCD diffractometer
Absorption correction: multi-scan (*SADABS*; Sheldrick, 2002)
$T_{\rm min}$ = 0.47, $T_{\rm max}$ = 0.95
18651 measured reflections
3762 independent reflections
2578 reflections with $I > 2\sigma(I)$
$R_{\rm int}$ = 0.044

Refinement

$R[F^2 > 2\sigma(F^2)]$ = 0.040
$wR(F^2)$ = 0.091
S = 1.04
3762 reflections
205 parameters
H-atom parameters constrained
$\Delta\rho_{\rm max}$ = 0.28 e Å^{-3}
$\Delta\rho_{\rm min}$ = −0.33 e Å^{-3}

Compound (I*b*), at 210 K

Crystal data

[Co(C$_5$H$_7$O$_2$)$_3$]
M_r = 356.25
Monoclinic, $P2_1/c$
a = 13.7708 (8) Å
b = 7.4195 (3) Å
c = 16.1242 (7) Å
β = 98.455 (2)°
V = 1629.54 (14) Å^3
Z = 4
Mo $K\alpha$ radiation
μ = 1.08 mm^{-1}
T = 210 (2) K
0.23 × 0.15 × 0.05 mm

Data collection

Nonius KappaCCD diffractometer
Absorption correction: multi-scan (*SADABS*; Sheldrick, 2002)
$T_{\min} = 0.52$, $T_{\max} = 0.95$
18555 measured reflections
3741 independent reflections
2680 reflections with $I > 2\sigma(I)$
$R_{\rm int} = 0.042$

Refinement

$R[F^2 > 2\sigma(F^2)] = 0.039$
$wR(F^2) = 0.087$
$S = 1.07$
3741 reflections
205 parameters
H-atom parameters constrained
$\Delta\rho_{\max} = 0.28$ e Å^{-3}
$\Delta\rho_{\min} = -0.35$ e Å^{-3}

Compound (**I***c*), at 180 K

Crystal data

$[Co(C_5H_7O_2)_3]$
$M_r = 356.25$
Monoclinic, $P2_1/c$
$a = 13.7338$ (6) Å
$b = 7.4070$ (3) Å
$c = 16.0959$ (7) Å
$\beta = 98.467$ (1)°
$V = 1619.53$ (12) Å^3
$Z = 4$
Mo $K\alpha$ radiation
$\mu = 1.08$ mm^{-1}
$T = 180$ (2) K
0.23 × 0.15 × 0.05 mm

Data collection

Nonius KappaCCD diffractometer
Absorption correction: multi-scan (*SADABS*; Sheldrick, 2002)
$T_{\min} = 0.51$, $T_{\max} = 0.95$
18433 measured reflections
3713 independent reflections
2765 reflections with $I > 2\sigma(I)$
$R_{\rm int} = 0.039$

Refinement

$R[F^2 > 2\sigma(F^2)] = 0.036$
$wR(F^2) = 0.079$
$S = 1.04$
3713 reflections
205 parameters
H-atom parameters constrained
$\Delta\rho_{\max} = 0.29$ e Å^{-3}
$\Delta\rho_{\min} = -0.35$ e Å^{-3}

Compound (**I***d*), at 150 K

Crystal data

$[Co(C_5H_7O_2)_3]$
$M_r = 356.25$
Monoclinic, $P2_1/c$
$a = 13.6927$ (6) Å
$b = 7.3920$ (3) Å
$c = 16.0641$ (6) Å
$\beta = 98.499$ (2)°
$V = 1608.11$ (11) Å^3
$Z = 4$
Mo $K\alpha$ radiation
$\mu = 1.09$ mm^{-1}
$T = 150$ (2) K
0.23 × 0.15 × 0.05 mm

Data collection

Nonius KappaCCD diffractometer
Absorption correction: multi-scan (*SADABS*; Sheldrick, 2002)
$T_{\min} = 0.47$, $T_{\max} = 0.95$
18370 measured reflections
3698 independent reflections
2812 reflections with $I > 2\sigma(I)$
$R_{\rm int} = 0.043$

Refinement

$R[F^2 > 2\sigma(F^2)] = 0.035$
$wR(F^2) = 0.080$
$S = 1.03$
3698 reflections
205 parameters
H-atom parameters constrained
$\Delta\rho_{\max} = 0.31$ e Å^{-3}
$\Delta\rho_{\min} = -0.42$ e Å^{-3}

Compound (**I***e*), at 110 K

Crystal data

$[Co(C_5H_7O_2)_3]$
$M_r = 356.25$
Monoclinic, $P2_1/c$
$a = 13.6376$ (5) Å
$b = 7.3758$ (3) Å
$c = 16.0446$ (9) Å
$\beta = 98.594$ (2)°
$V = 1595.78$ (12) Å^3
$Z = 4$
Mo $K\alpha$ radiation
$\mu = 1.10$ mm^{-1}
$T = 110$ (2) K
0.23 × 0.15 × 0.05 mm

Data collection

Nonius KappaCCD diffractometer
Absorption correction: multi-scan (*SADABS*; Sheldrick, 2002)
$T_{\min} = 0.57$, $T_{\max} = 0.95$
27696 measured reflections
3656 independent reflections
3018 reflections with $I > 2\sigma(I)$
$R_{\rm int} = 0.040$

Refinement

$R[F^2 > 2\sigma(F^2)] = 0.029$
$wR(F^2) = 0.065$
$S = 1.06$
3656 reflections
205 parameters
H-atom parameters constrained
$\Delta\rho_{\max} = 0.32$ e Å^{-3}
$\Delta\rho_{\min} = -0.37$ e Å^{-3}

Table 1
Cell parameters (Å, °) of the known room-temperature Co(acac)$_3$ crystal structure determinations.

a	b	c	β	Reference
14.160	7.480	16.430	98.68	Padmanabhan (1958)
14.25 (3)	7.50 (2)	16.38 (3)	99 (1)	Shkol'nikova (1959)
13.951 (9)	7.470 (5)	16.222 (11)	98.48 (8)	Hon & Pfluger (1973)
13.90 (7)	7.47 (4)	16.21 (7)	98.4 (1)	Krüger & Reynhardt (1974)
13.8663 (15)	7.4599 (5)	16.1874 (9)	98.409 (5)	Present study

Table 2
Tensor components of the thermal expansion (10^{-6} K^{-1}).

Standard uncertainties are underestimated because calculated θ values were used (see *Comment*).

T (K)	α_{11}	α_{22}	α_{33}	α_{12}	α_{13}	α_{23}
290–270	80.79 (3)	76.54 (4)	53.01 (17)	0	−4.34 (12)	0
270–250	94.35 (2)	75.41 (3)	57.17 (13)	0	−3.63 (9)	0
250–230	94.51 (3)	75.45 (4)	53.85 (17)	0	−4.30 (11)	0
230–210	101.56 (2)	72.40 (3)	59.04 (13)	0	5.25 (9)	0
210–190	89.56 (3)	67.08 (4)	49.23 (18)	0	2.46 (12)	0
190–170	107.55 (2)	52.85 (3)	56.87 (14)	0	10.89 (10)	0
170–150	100.83 (2)	74.01 (3)	57.90 (12)	0	5.32 (8)	0
150–130	108.88 (2)	50.06 (3)	52.58 (10)	0	9.17 (7)	0
130–110	96.35 (2)	61.16 (3)	47.50 (11)	0	7.34 (7)	0

Table 3
Eigenvalues (10^{-6} K^{-1}) and eigenvectors of the thermal expansion tensor.

T (K)	Principal axis	Eigenvalue	Eigenvector		
290–270	α_1	52.3	0.1513	0	0.9885
	α_2	76.5	0	1.0	0
	α_3	81.5	−0.9886	0.0	0.1508
270–250	α_1	56.8	0.0965	0.0	0.9953
	α_2	75.4	0	1.0	0
	α_3	94.7	−0.9954	0	0.0960
250–230	α_1	53.4	0.1043	0	0.9945
	α_2	75.5	0	1.0	0
	α_3	95.0	−0.9946	0	0.1039
230–210	α_1	58.4	−0.1211	0	0.9926
	α_2	72.4	0	−1.0	0
	α_3	102.2	0.9927	0	0.1207
210–190	α_1	49.1	−0.0610	0	0.9981
	α_2	67.1	0	−1.0	0
	α_3	89.7	0.9982	0	0.0606
190–170	α_1	52.8	0	−1.0	0
	α_2	54.6	−0.2019	0	0.9794
	α_3	109.8	0.9795	0	0.2015
170–150	α_1	57.3	−0.1215	0	0.9926
	α_2	74.0	0	−1.0	0
	α_3	101.5	0.9926	0	0.1211
150–130	α_1	50.1	0	−1.0	0
	α_2	51.1	−0.1570	0	0.9876
	α_3	110.3	0.9876	0	0.1567
130–110	α_1	46.4	−0.1456	0	0.9893
	α_2	61.2	0	−1.0	0
	α_3	97.4	0.9894	0	0.1453

Table 4
Hydrogen-bond geometry (Å, °) for (I*a*) (240 K) to (I*e*) (110 K).

	D—H···*A*	*D*—H	H···*A*	*D*···*A*	*D*—H···*A*
(I*a*)	C1—H1*A*···O4^{i}	0.97	2.54	3.513 (3)	178
(I*b*)	C1—H1*A*···O4^{i}	0.97	2.54	3.512 (3)	179
(I*c*)	C1—H1*A*···O4^{i}	0.98	2.53	3.507 (3)	178
(I*d*)	C1—H1*A*···O4^{i}	0.98	2.52	3.501 (3)	179
(I*e*)	C1—H1*A*···O4^{i}	0.98	2.52	3.497 (2)	180
(I*a*)	C6—H6*B*···O6^{ii}	0.97	2.53	3.492 (3)	172
(I*b*)	C6—H6*B*···O6^{ii}	0.97	2.52	3.478 (3)	172
(I*c*)	C6—H6*B*···O6^{ii}	0.98	2.50	3.467 (3)	172
(I*d*)	C6—H6*B*···O6^{ii}	0.98	2.48	3.455 (3)	171
(I*e*)	C6—H6*B*···O6^{ii}	0.98	2.47	3.442 (2)	171
(I*a*)	C11—H11*B*···O1^{iii}	0.97	2.78	3.743 (4)	175
(I*b*)	C11—H11*B*···O1^{iii}	0.97	2.75	3.716 (4)	175
(I*c*)	C11—H11*B*···O1^{iii}	0.98	2.71	3.690 (3)	174
(I*d*)	C11—H11*B*···O1^{iii}	0.98	2.68	3.660 (3)	177
(I*e*)	C11—H11*B*···O1^{iii}	0.98	2.65	3.629 (2)	178

Symmetry codes: (i) $x, y+1, z$; (ii) $x, -y+\frac{1}{2}, z-\frac{1}{2}$; (iii) $-x, -y+1, -z+1$.

Table 5
Co—O bond lengths (Å) for (I*a*) (240 K) to (I*e*) (110 K).

Co—O	(I*a*)	(I*b*)	(I*c*)	(I*d*)	(I*e*)
Co1—O5	1.8746 (18)	1.8748 (17)	1.8762 (16)	1.8766 (15)	1.8770 (12)
Co1—O6	1.8798 (17)	1.8815 (16)	1.8813 (15)	1.8801 (14)	1.8827 (12)
Co1—O3	1.8826 (17)	1.8834 (16)	1.8851 (15)	1.8835 (14)	1.8859 (12)
Co1—O4	1.8841 (17)	1.8846 (16)	1.8853 (15)	1.8856 (14)	1.8865 (12)
Co1—O2	1.8872 (17)	1.8878 (16)	1.8893 (15)	1.8899 (14)	1.8906 (12)
Co1—O1	1.8892 (17)	1.8884 (16)	1.8902 (15)	1.8912 (14)	1.8913 (12)

The crystal structure determinations of (I*a*)–(I*e*) were all carried out on the same crystal, which was mounted on a glass capillary with perfluoro polyether oil (Kottke & Stalke, 1993). The X-ray intensities of (I*a*)–(I*d*) were obtained with an exposure time of 40 s per frame and a rotation angle of 1°. 258 φ and 125 ω scans were measured. The X-ray intensities of (I*e*) were obtained with two different exposure times and rotation angles of 1°. 258 φ and 323 ω scans were measured with an exposure time of 60 s per frame and 173 φ scans with an exposure time of 12 s per frame.

For the structure solution of (I*a*), coordinates were taken from those of α-Al(acac)$_3$ (von Chrzanowski *et al.*, 2007); subsequently, coordinates were taken from (I*a*) for (I*b*), from (I*b*) for (I*c*), from (I*c*) for (I*d*) and from (I*d*) for (I*e*). All H atoms were introduced in geometrically idealized positions, refined with a riding model and subsequently confirmed in a difference Fourier map. Their $U_{\rm iso}$(H) values were set at $1.2U_{\rm eq}$(C) for H atoms of the central CH groups and at $1.5U_{\rm eq}$(C) for methyl H atoms.

Because the above-mentioned oil mounting technique is not suitable for ambient temperatures, a second, different, crystal was selected and mounted with Super Glue for the cell-parameter determinations. The detector position was kept fixed and the *Phi*/*Phi-Chi* routine (Duisenberg *et al.*, 2000) was used.

For all determinations, data collection: *COLLECT* (Nonius, 1999); cell refinement: *PEAKREF* (Schreurs, 2005); data reduction: *EVALCCD* (Duisenberg *et al.*, 2003) and *SADABS* (Sheldrick, 2002); program(s) used to refine structure: *SHELXL97* (Sheldrick, 1997); molecular graphics: *PLATON* (Spek, 2003); software used to prepare material for publication: manual editing of *SHELXL97* output.

This work was supported by the Council for Chemical Sciences of the Netherlands Organization for Scientific Research (CW–NWO).

Supplementary data for this paper are available from the IUCr electronic archives (Reference: GZ3091). Services for accessing these data are described at the back of the journal.

References

Alekseev, A. V., Gromilov, S. A., Baidina, I. A., Stabnikov, P. A. & Prokuda, O. V. (2006). *Zh. Strukt. Khim.* **47**, 324–331.

Astbury, W. T. & Morgan, G. T. (1926). *Proc. R. Soc. London Ser. A*, **112**, 448–467.

Boldyreva, E., Kivikoski, J. & Howard, J. A. K. (1997). *Acta Cryst.* B**53**, 394–404.

Chrzanowski, L. S. von, Lutz, M. & Spek, A. L. (2006). *Acta Cryst.* E**62**, m3318–m3320.

Chrzanowski, L. S. von, Lutz, M. & Spek, A. L. (2007). *Acta Cryst.* C**63**, m129–m134.

Diaz-Acosta, I., Baker, J., Hinton, J. F. & Pulay, P. (2003). *Spectrochim. Acta Part A*, **59**, 363–377.

Duisenberg, A. J. M., Hooft, R. W. W., Schreurs, A. M. M. & Kroon, J. (2000). *J. Appl. Cryst.* **33**, 893–898.

Duisenberg, A. J. M., Kroon-Batenburg, L. M. J. & Schreurs, A. M. M. (2003). *J. Appl. Cryst.* **36**, 220–229.

Geremia, S. & Demitri, N. (2005). *J. Chem. Educ.* **82**, 460–465.

Herbstein, F. H. (2000). *Acta Cryst.* B**56**, 547–557.

Hon, P. K. & Pfluger, C. E. (1973). *J. Coord. Chem.* **3**, 67–76.

Hummel, W., Hauser, J. & Bürgi, H. B. (1990). *J. Mol. Graph.* **8**, 214–220.

Jessen, S. M. & Küppers, H. (1991). *J. Appl. Cryst.* **24**, 239–242.

Kitaigorodsky, A. I. (1973). *Molecular Crystals and Molecules*, pp. 337–380. New York: Academic Press.

Kottke, T. & Stalke, D. (1993). *J. Appl. Cryst.* **26**, 615–619.

Krüger, G. J. & Reynhardt, E. C. (1974). *Acta Cryst.* B**30**, 822–824.

Nonius (1999). *COLLECT*. Nonius BV, Delft, The Netherlands.

Padmanabhan, V. M. (1958). *Proc. Indian Acad. Sci. A*, **47**, 329–334.

Pilati, T. & Forni, A. (1998). *J. Appl. Cryst.* **31**, 503–504.

Salud, J., Barrio, M., López, D. O., Tamarit, J. L. & Alcobé, X. (1998). *J. Appl. Cryst.* **31**, 748–757.

Schomaker, V. & Trueblood, K. N. (1998). *Acta Cryst.* B**54**, 507–514.

Schreurs, A. M. M. (2005). *PEAKREF*. Utrecht University, The Netherlands.

Sheldrick, G. M. (1997). *SHELXL97*. University of Göttingen, Germany.

Sheldrick, G. M. (2002). *SADABS*. University of Göttingen, Germany.

Shkol'nikova, L. M. (1959). *Kristallografiya*, **4**, 419–420.

Spek, A. L. (2003). *J. Appl. Cryst.* **36**, 7–13.

Wiberg, N. (1985). *Holleman-Wiberg Lehrbuch der Anorganischen Chemie*, 91–100 Auflage, pp. 979–983. Berlin: Walter de Gruyter. (In German.)